Title: Synchronous multipass spinning of oblique-bottom shape

Authors: Hirohiko Arai* and Tatsuru Kanazawa**

Affiliations:

* National Institute of Advanced Industrial Science and Technology (AIST)

1-2-1 Namiki, Tsukuba, Ibaraki 305-8564 Japan

** The University of Tsukuba

1-1-1 Tennodai, Tsukuba, Ibaraki 305-8577 Japan

Email: h.arai@aist.go.jp

Advanced Manufacturing Research Institute

National Institute of Advanced Industrial Science and Technology (AIST)

1-2-1 Namiki, Tsukuba, Ibaraki 305-8564 Japan

Journal of Materials Processing Technology 260 (2018): 66-76.

https://www.sciencedirect.com/science/article/pii/S0924013618301936

https://doi.org/10.1016/j.jmatprotec.2018.04.046

Abstract: Recently, various methods for the metal spinning of noncircular shapes have been proposed to overcome the limitation of its application range. In this study, a metal spinning method for noncircular shapes with oblique bottoms is proposed. This method is a combination of synchronous spinning and multipass spinning, in which the roller is synchronized with the mandrel rotation to track a noncircular cross section while the workpiece is gradually deformed without much thinning through some paths of the roller. The roller trajectory is calculated by linear interpolation in the radial direction and axial direction between the inclined blank shape and the inclined cross section of the product. A circular cup and square cup with an oblique bottom and vertical side walls are successfully spun using this method. As the wall thickness locally increases at the side edges of the square cup, the thickness distribution is equalized by using an intermediate circular shape. This method interpolates the roller trajectory between the blank shape and intermediate shape and between the intermediate shape and the product. The difference in the wall thickness is reduced since the square shape is formed via a cylindrical shape. In addition, the effect of the process parameters on the forming results is experimentally investigated.
Keywords: Metal Forming; Metal Spinning; Incremental Forming; Tool Trajectory; Linear Interpolation

1. Introduction

Metal Spinning is a plastic forming method for circular shapes in which a roller is pressed against a metal sheet or metal tube rotating on a lathe. It is widely used as a method of manufacturing round metal parts and products, such as automobile parts, aerospace parts, pressure vessels, liquid containers, funnels, nozzles, and parabolic antennas. Compared with stamping or deep drawing, it is more suitable for high-mix low-volume production because of its low tooling cost.

The recent development of metal spinning methods has also enabled the forming of various noncircular shapes to overcome the limitation of the application range of metal spinning. These new methods are generally classified into two types: synchronous spinning and force-controlled spinning. In synchronous spinning, the radial displacement of the roller actively synchronizes with the rotation angle of the workpiece. The forming roller moves in the radial direction in accordance with the rotation angle of the workpiece so that the trajectory of the contact point between the roller and the workpiece becomes the target cross-section shape. The sectional shape is changed along the axial direction and the whole workpiece is formed into the target shape.

Amano and Tamura (1984) formed an elliptic cone from an aluminum

sheet by moving a forming roller mechanically synchronized with the rotation of a spindle and pushing the material onto an elliptic mandrel. A mechanical cam, gears, and a lever were used to drive the roller. Xia et al. (2010) also used gears and a three-dimensional cam in a method called "profile driving" to fit the motion of a forming roller to the mandrel shape, and formed cone shapes with noncircular cross sections.

Shimizu (2010) adopted the numerical control of stepping motors to move a roller in synchronous spinning and formed elliptic and square cones from aluminum sheets. Arai et al. (2005) conducted noncircular tube necking of elliptic and eccentric cross sections by synchronous spinning using a CNC spinning machine with a spindle axis driven by a servo motor. The use of computer control in driving the forming roller and the spindle rotation makes complicated mechanisms for the synchronization of the roller and spindle unnecessary. It reduces the cost of the dedicated cam for each cross-section shape and can make the noncircular spinning process more flexible.

Another type of noncircular spinning is force-controlled spinning, in which a noncircular mandrel is used and the pushing force of a roller is controlled so that the material is pushed onto the mandrel. As the mandrel rotates, the roller follows the cross-section shape of the mandrel to maintain an appropriate pushing force. Awiszus and Meyer (2005) used two rollers

that pulled each other by strong springs, which pinched the workpiece and the noncircular mandrel. A semi-triangle cone was formed from a steel sheet by this method. Arai (2005) applied force-feedback control for noncircular metal spinning. A force/torque sensor was attached at the base of the forming roller and the pushing force was fed back to a computer to control servo motors so as to keep the pushing force constant. Arai (2006) used linear servo motors to drive a roller to realize faster motion of the roller and reduced the forming time of noncircular shapes.

The previous methods described above except for that of Arai et al. (2005) spun the target shape from a sheet blank with just one pass of the roller along the mandrel surface, and consequently they are classified into shear spinning or simple conventional spinning. Shear spinning reduces the wall thickness from the original thickness of the blank, while the outer diameter of the blank does not change during the forming. The wall thickness t of the product is

$$t = t_0 \sin\alpha , \qquad (1)$$

where the thickness of the blank is t_0 and the half cone angle is α. This relation is called the "sine law". When the half cone angle is zero, i.e., in the case of a vertical wall, the wall thickness after forming becomes zero from Equation (1) and fracture occurs. Therefore, a product with vertical walls

cannot be formed by shear spinning from a metal sheet.

In contrast, the multipass (conventional) spinning process for circular shapes presses a metal sheet onto a mandrel with multiple tool paths. A forming roller moves back and forth between the mandrel surface and the periphery of the workpiece. The blank gradually deforms closer to the mandrel shape with less thinning of the side wall than that predicted by the sine law. Simple conventional spinning is a special case when a single path is used, but it only allows a shallow shape when the diameter of the blank is close to that of the mandrel.

Multipass spinning has been expanded to noncircular shapes in some studies. Härtel and Laue (2016) formed a tripod shape via two roller paths and optimized the forming conditions on the basis of FEM simulation. A circular cone was spun as a preformed shape from a flat blank in the first path, and then a roller pushed the workpiece into the final shape of the tripod mandrel, which was difficult to spin with a single pass owing to wrinkling. Sugita and Arai (2015) proposed synchronous multipass spinning to spin noncircular shapes with vertical walls such as a square cup (Figure 1). Synchronous multipass spinning is a combination of multipass spinning, which progressively performs forming from a flat blank in multiple steps, and synchronous spinning, which controls the roller displacement in

the radial direction by synchronizing with workpiece rotation angle. Although the three-dimensional tool trajectory of multiple paths appears to be rather complicated, it can be easily calculated from the mandrel shape, the blank shape, and the normalized path profile. Music and Allwood (2011) found that the contact force between the workpiece and mandrel in multipass spinning is locally distributed in only several small areas. On the basis of this result, a spinning machine for noncircular shapes was developed that supports the workpiece using three movable rollers instead of the mandrel.

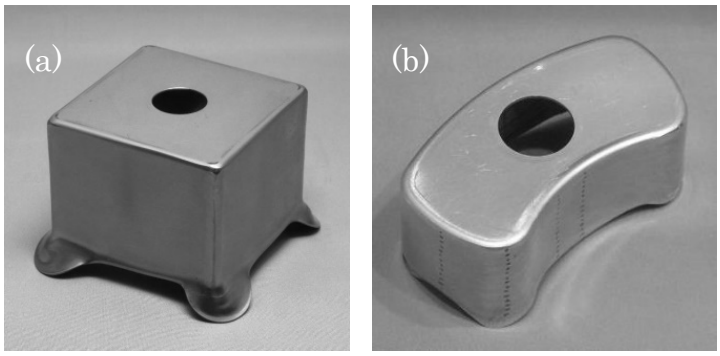

Figure 1 Photographs of noncircular shapes with vertical walls formed by synchronous multipass spinning.

(a) square cup, cold-rolled steel [Arai (2013)]

(b) concave cross section, aluminum [Sugita and Arai (2011)]

From a different viewpoint, all the methods described above deal with non-oblique spinning. The cross section being formed is always perpendicular to the spindle axis. In contrast, several spinning methods were developed to form inclined and curbed shapes. Irie (2001) developed a spinning machine for the tube necking of oblique shapes. Planetary rollers driven by a spindle rotate around the workpiece and change the rotating radius so as to neck the tube end, while the workpiece is rotated relative to the spindle axis to obtain an oblique end. Xia et al. (2012) simulated the forming process of this method and investigated the effect of various forming parameters. Sekiguchi and Arai (2010) carried out oblique synchronous spinning of a metal sheet. This method expands the synchronous spinning method to enable the forming of oblique and curved shell shapes. The roller motion in the axial direction as well as that in the radial direction synchronizes with the workpiece rotation (Figure 2). The curved shape is defined by continuously changing the inclination angle of the cross section. As this method is a type of shear spinning, shapes with vertical walls cannot be formed owing to the sine law.

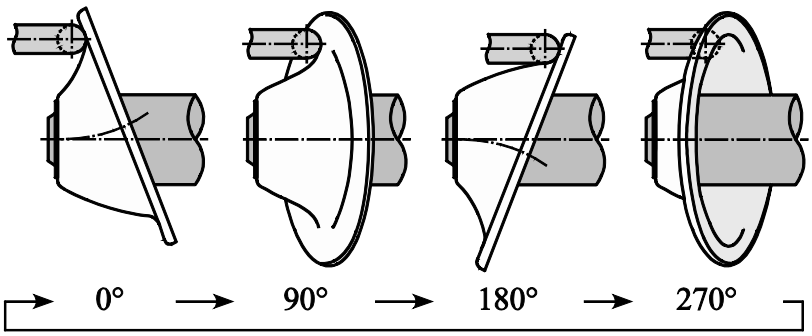

Figure 2　Oblique synchronous spinning performed by Sekiguchi and Arai (2010).

This paper deals with target cup shapes that simultaneously have i) a noncircular cross section, ii) an oblique bottom and iii) vertical side walls. These shapes cannot be formed from a sheet blank by the previous methods reviewed above.　Three types of roller motion, i) radial motion synchronized with the spindle rotation to follow the noncircular cross section, ii) axial motion synchronized with the spindle rotation to follow the oblique bottom and blank and iii) step-by-step tool paths that change a flat blank to vertical walls, should be unified to a tool trajectory to achieve each feature of the target shape.　For this purpose, the synchronous multipass spinning method in Sugita and Arai (2015) is extended to afford synchronous motion in the axial direction.

Section 2 describes how to calculate the tool trajectory in this method. Section 3 describes forming experiments on circular and square cup shapes

with an oblique bottom. Section 4 presents the forming method via an intermediate shape to avoid material concentration at the corners of the square cup. Section 5 experimentally shows the effect of the process parameters on the forming result. Section 6 summarizes the findings obtained in this study.

2. Method for calculation of tool trajectory

2.1 Tool trajectory in synchronous multipass spinning

Before explaining oblique synchronous multipass spinning, the tool trajectory calculation for synchronous multipass spinning in Sugita and Arai (2014) is reviewed here. In the spinning of a noncircular shape, the movement of the roller is represented by three-dimensional data in the axial direction and the radial direction and the rotation angle of the workpiece. A three-dimensional tool trajectory should be planned from the initial flat blank to the final shape of the product.

To closely fit the material onto the mandrel in the final state, the tool trajectory should move along the completed shape of the product. In the initial state, the tool trajectory should move along the blank shape from the center to the periphery. On the other hand, it is desirable that an operator can set the trajectory intuitively and graphically based on similar intuition

to that in conventional circular spinning, so that the trajectory can be adjusted on the basis of trial and error. Considering these requirements, the tool trajectory is generated by the following three steps.

1) Defining the product shape and blank shape

2) Setting the normalized tool path

3) Calculating the tool trajectory by linear interpolation

The shape data of the product are expressed by the tool position at which the roller comes in contact with the product surface. The product shape is composed of several major cross sections around the spindle axis. One revolution of each cross section is divided into many angles, and the contact position at each angle is treated as a shape data element. The axial and radial components of the product shape are represented as x_{p_k} and $y_{p\_k}(\theta)$ $(k = 1, \cdots, n)$, respectively, where θ is the rotation angle of the spindle and n is the number of the representative cross section. The blank shape is also defined as $y_b(\theta)$ from the tool position where the roller comes in contact with the periphery of the blank.

Next, multiple tool paths are defined on a virtual two-dimensional plane (Figure 3 (a)). The virtual plane is normalized from 0 to 1 in the axial direction s_x and radial direction s_y of the workpiece. $s_x = 0$ represents the upper end of the product and $s_x = 1$ represents the lower end. When

$s_y = 1$, the roller moves along the periphery of the blank, and when $s_y = 0$ it moves along the product surface.

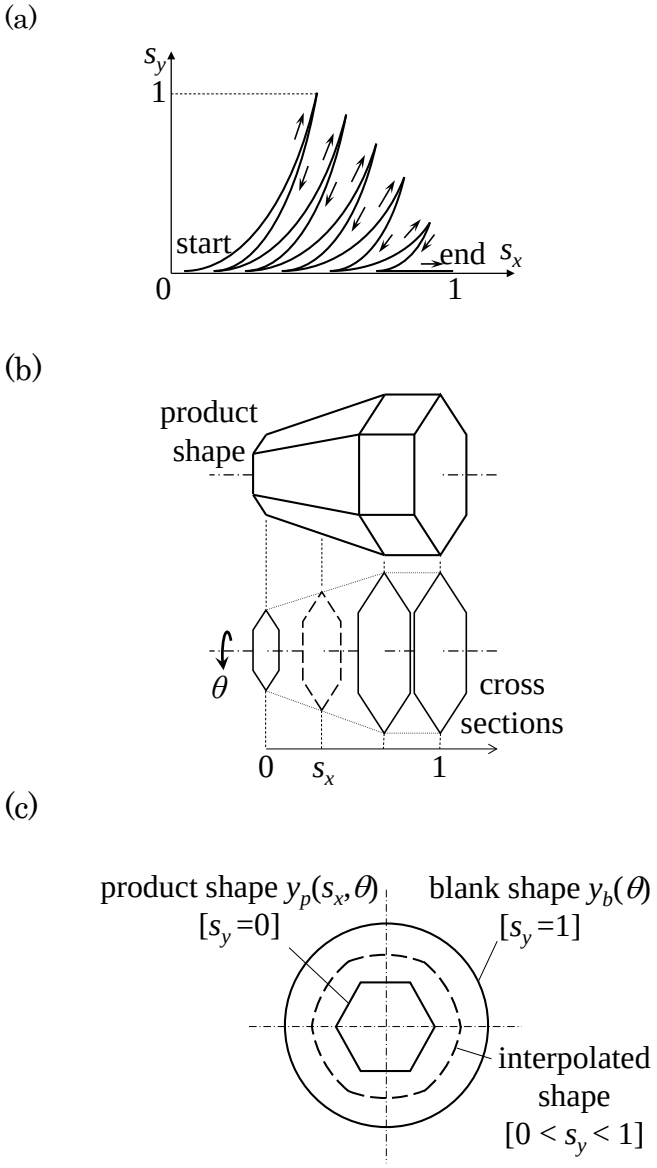

Figure 3　Tool trajectory calculation in synchronous multipass spinning.

(a) normalized paths in two-dimensional virtual plane

(b) interpolation in axial direction

(c) interpolation in radial direction

A straight path, a curved path, and a force-controlled path are used as elements of the multiple tool paths. The straight path is the straight line that connects the start point and the end point. The curved path is a circular arc connecting the start point and the end point. The curved path is represented by Equation (2) when the path is directed from the mandrel to the blank edge, and represented by Equation (3) when the path is in the opposite direction, where the start point is (q_{xs}, q_{ys}), the end point is (q_{xe}, q_{ye}), and the time is t $(0 \le t \le 1)$.

$$\begin{cases} s_x(t) = q_{xs} + (q_{xe} - q_{xs}) \dfrac{\cos\alpha - \cos((\beta - \alpha)t + \alpha)}{\cos\alpha - \cos\beta} \\ s_y(t) = q_{ys} + (q_{ye} - q_{ys}) \dfrac{\sin((\beta - \alpha)t + \alpha) - \sin\alpha}{\sin\beta - \sin\alpha} \end{cases} \tag{2}$$

$$\begin{cases} s_x(t) = q_{xs} + (q_{xe} - q_{xs}) \dfrac{\sin((\beta - \alpha)t + \alpha) - \sin\alpha}{\sin\beta - \sin\alpha} \\ s_y(t) = q_{ys} + (q_{ye} - q_{ys}) \dfrac{\cos\alpha - \cos((\beta - \alpha)t + \alpha)}{\cos\alpha - \cos\beta} \end{cases} \tag{3}$$

$$(\alpha = 15°, \beta = 75°)$$

The force-controlled path is a path that controls the pushing force of the roller with the target force given in the radial direction of the mandrel while feeding at a constant speed in the axial direction of the mandrel. When the roller is position-controlled, it is necessary to follow a trajectory near the mandrel while considering the thickness of the product. Therefore, precise

measurement and positioning accuracy are required so that the workpiece can tightly fit the mandrel. It is possible to perform precise forming by making an approximate shape by position control and then pressing the workpiece onto the mandrel using force control to complete the forming. A formable set of multiple paths is composed of these three types of path elements so as not to cause wrinkles and fractures.

Finally, the actual tool position corresponding to a point (s_x, s_y) on the normalized tool path (Figure 3 (a)) is calculated by interpolation. The tool position x_t in the axial direction is obtained from s_x by

$$x_t = x_{p\_1} + (x_{p\_n} - x_{p\_1})s_x, \qquad (4)$$

where x_{p_1} is the axial position of the upper end of the product and x_{p_n} is that of the lower end.

The shape of the product is defined by some representative cross sections, and the cross-section shape corresponding to the axial displacement s_x on the normalized path is calculated using s_x as an interpolation coefficient (Figure 3 (b)). The cross-section shape $y_p(s_x, \theta)$ is generated by linear interpolation of cross sections $y_{p\_k+1}(\theta)$ and $y_{p\_k}(\theta)$, which are the neighboring cross sections to x_t.

$$y_p(s_x, \theta) = s_k(s_x) y_{p\_k+1}(\theta) + (1 - s_k(s_x)) y_{p\_k}(\theta) \qquad (5)$$

Here $s_k(s_x)$ is a coefficient used in the interpolation of $y_{p\_k+1}(\theta)$ and

$y_{p\_k}(\theta)$ at s_x.

Then the product cross section and the periphery of the blank are interpolated using s_y as an interpolation coefficient to obtain the cross-section shape in the intermediate state (Figure 3 (c)). The radial tool position y_t is calculated from the cross-section shape $y_p(s_x,\theta)$ and the blank shape $y_b(\theta)$ as follows:

$$y_t = s_y y_b(\theta) + (1-s_y) y_p(s_x,\theta). \quad (6)$$

These tool position calculations are sequentially performed to generate the whole tool trajectory.

As the tool path is defined as dimensionless normalized data in this method, it is possible to handle the tool path, the product shape, and the blank shape independently. For this reason, once a successful tool path is obtained, it is possible to exchange the product shape or the blank shape unless these shapes are considerably different.

2.2 Tool trajectory for oblique multipass spinning

In the method in the previous subsection, it is not possible to spin a shape with an oblique bottom because the axial direction is assumed to proceed constantly. To deal with an oblique shape, the roller should move in the axial direction in response to the rotation to maintain contact with the workpiece (Figure 4). The shape data of the product are represented by a

combination of the axial and radial displacements as $(x_{p\_k}(\theta), y_{p\_k}(\theta))$ $(k = 1, \cdots, n)$. Each point is on the inclined cross section of the product. The blank shape is also represented as $(x_{b\_k}(\theta), y_{b\_k}(\theta))$ $(k = 1, \cdots, n)$.

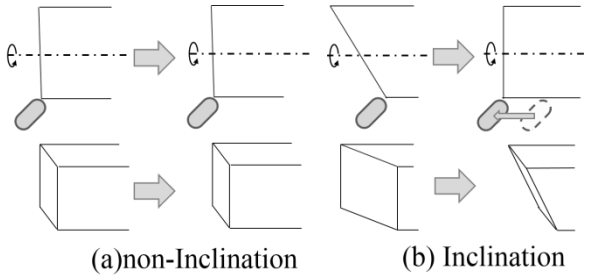

Figure 4 Contact between roller and workpiece in oblique and non-oblique spinning.

As the axial direction also changes with rotation, interpolation in the axial direction in accordance with the rotation is necessary as well as in the radial direction. Instead of Equation (6), the roller position (x_t, y_t) corresponding to (s_x, s_y) is calculated as

$$\begin{cases} x_t = s_y x_b(s_x, \theta) + (1 - s_y) x_p(s_x, \theta) \\ y_t = s_y y_b(s_x, \theta) + (1 - s_y) y_p(s_x, \theta) \end{cases} . \quad (7)$$

In Equation (7), the roller positions x_t and y_t both change in accordance with the workpiece angle, and forming can be performed by following the inclination of the product shape.

3. Forming Experiment

A cylindrical cup and square cup with an oblique bottom were experimentally formed by the proposed method. A force-controlled three-axis spinning machine was used to perform measurement and forming using force control.

3.1 Experimental setup

The force-controlled spinning machine is depicted in Figure 5. The roller is mounted on an XY table driven by 400 W servo motors and ball screws of 5 mm/rev lead. The spindle axis is driven by a 400 W servo motor with a 1/21 planetary gear. Each servo motor is equipped with a rotary encoder to measure the position and angle. The roller is mounted via a six-axis force sensor with a 45° offset angle relative to the spindle axis. The diameter of the roller is 70 mm, the radius of roundness is 8 mm, and the material is alloy tool steel (SKD 11).

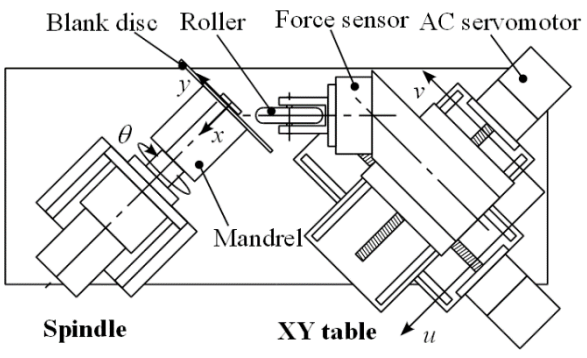

Figure 5 Force-controlled spinning machine.

3.2 Cylindrical cup with oblique bottom

First, a forming experiment on a cylindrical cup with an oblique bottom was conducted. A pure aluminum (A1050 - H24) circular sheet with a diameter of 140 mm and a thickness of 1.5 mm was used as a blank. The mandrel, shown in Figure 6, had a cylindrical shape with a diameter of 75 mm, a height of 50 mm, and a bottom inclination angle of 20°. The inclination angle was determined to avoid interference between the roller holder and the workpiece. The roller holder should not touch the inclined blank in the beginning of the process, while it should not touch the vertical side wall of the product at the end. It would be necessary to change the orientation of the roller holder during the spinning process to form a product with a more inclined bottom.

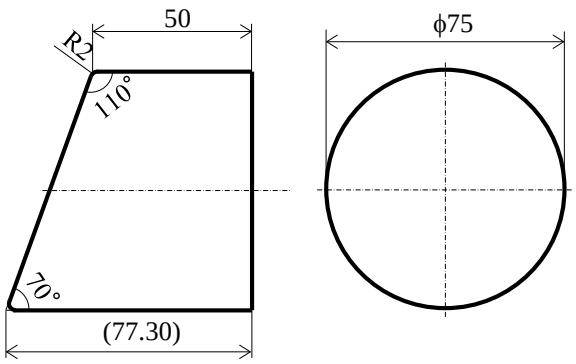

Figure 6 Mandrel for cylindrical cup with oblique bottom.

The shape data of the oblique cylindrical cup was composed of three cross sections, $(x_{p\_k}(\theta), y_{p\_k}(\theta))$ $(k = 1, 2, 3)$. While $(x_{p\_1}(\theta), y_{p\_1}(\theta))$ and $(x_{p\_2}(\theta), y_{p\_2}(\theta))$ were near the upper end of the mandrel and had an inclination angle of 20°, $(x_{p\_3}(\theta), y_{p\_3}(\theta))$ was near the lower end and perpendicular to the spindle axis. Thus, the inclination of the forming plane was gradually decreased from 20° to 0° by their interpolation.

Each cross section consisted of 90 contact points between the roller and the mandrel. The contact positions were automatically measured using force control. The roller slowly approached the mandrel towards the center of the cross section along an oblique plane including the cross section. The angle of approach relative to the radial direction was $\gamma = \tan^{-1}(\tan\varphi \cos\theta)$, where φ is the inclination angle of the cross section and θ is the spindle rotation angle, so that the contact point was on the oblique plane. When the force sensor detected the contact force with the mandrel, the roller stopped there and the roller position was recorded, adding a clearance equal to the blank thickness. Such contact measurement was repeated every 4° of mandrel rotation. Since the roller actually touched the mandrel during measurement, the compensation of the tool geometry was not necessary.

The tool path was composed of linear path, curved path, and force-controlled path elements as shown in Figure 7. Ten roundtrips of

curved/linear paths (black lines) were used to change the workpiece shape step by step and a final force-controlled path (gray line) was used to push the workpiece onto the mandrel. Although the force-controlled path did not actually have an s_y component, the roller moved along the product and it appeared to coincide with a linear path on the s_x axis. The rotation speed of the spindle axis was 60 rpm along the curved path and 7.5 rpm along the force-controlled path. The roller feed pitch was 1 mm/rev along the curved path and 0.5 mm/rev along the force-controlled path. The pushing force of the force-controlled path was 500 N. These forming conditions were selected such that wrinkles and fractures did not occur and the product was successfully formed. A multipurpose lubricant is sprayed on the blank.

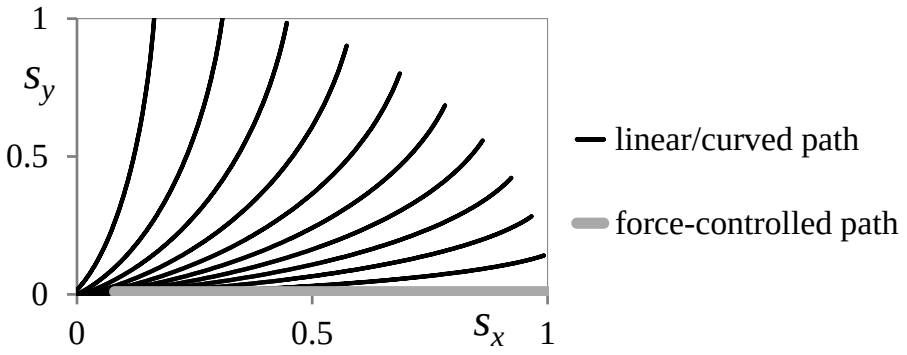

Figure 7 Normalized tool paths for cylindrical cup with oblique bottom.

Figure 8 shows a photograph of the spun product. The cylindrical cup was formed without a flange at the lower end. The flange was suppressed by reducing the angle of the forming plane to zero while approaching the lower end of the product (Figure 9). In a preliminary experiment, a large flange remained on one side when the inclination angle of the forming plane was constant throughout the forming.

The outer profile of the product was measured using a laser distance sensor. Figure 10 shows the circumferential profile of the formed product and Figure 11 shows the axial profile. The shape of the product fits the mandrel shape in Figure 10. The shape of the axial surface is almost smooth in Figure 11. The unevenness of about 0.1mm is considered to be the feed mark of the roller. Figure 12 shows the wall thickness distribution in the circumferential direction measured using a micrometer at a distance of 20 mm from the bottom. The angle between the side wall and the bottom was 110° when the spindle rotation angle was 0°. The side wall had almost uniform thickness irrespective of the bottom inclination.

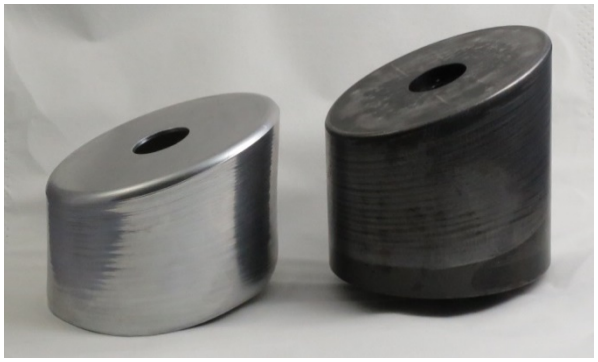

Figure 8　Photograph of formed product of cylindrical cup with oblique bottom (left: formed product, right: mandrel).

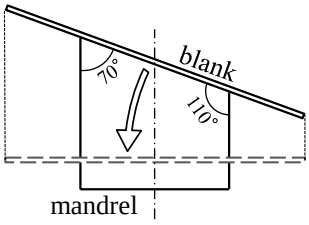

Figure 9　Change in inclination angle of forming plane.

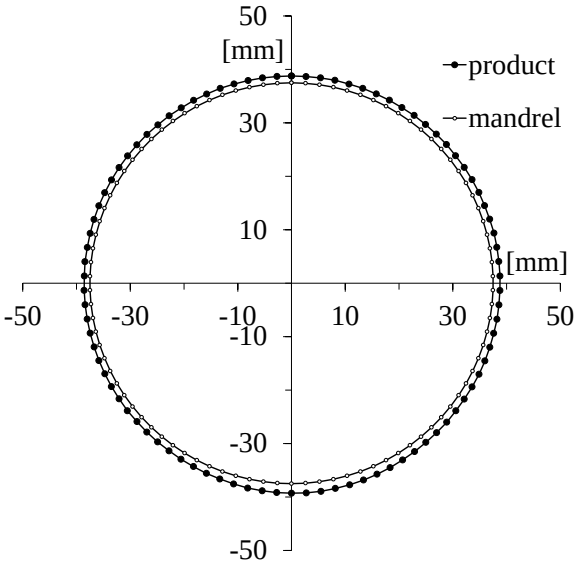

Figure 10　Circumferential profile of cylindrical cup with oblique bottom.

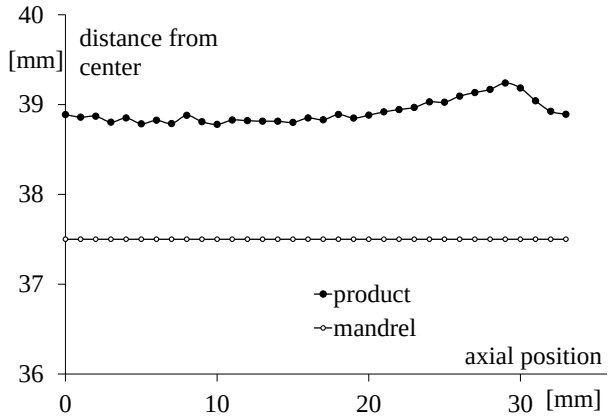

Figure 11　Axial profile of cylindrical cup with oblique bottom.

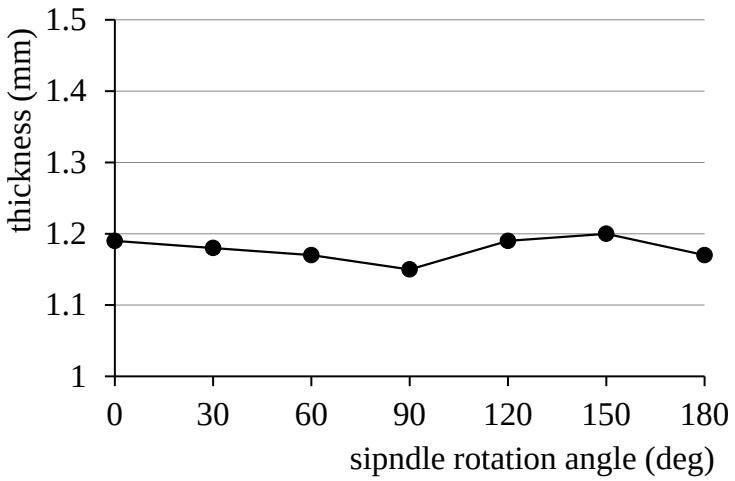

Figure 12　Wall thickness distribution of cylindrical cup with oblique bottom.

3.3 Square cup with oblique bottom

A forming experiment was conducted on a square cup with an oblique bottom.　The blank was the same aluminum sheet as that of the cylindrical cup.　The mandrel was a prism with a square cross section of 60 × 60 mm

and a height of 50 mm with an inclined bottom of 20° inclination (Figure 13).

The proposed oblique multipass spinning was conducted with the same machine. The contact position between the roller and the mandrel was measured at 90 points per rotation in the same way as Section 3.2. The cross section was at the upper end and the lower end of the mandrel and at two positions between them. The inclination angle of the forming plane was gradually decreased from 20° and was perpendicular to the spindle axis at the lower end. The tool path consisted of 20 roundtrips of curved/linear paths (black line) and a force-controlled path (gray line) as shown in Figure 14. The spindle rotation speed was 30 rpm for the curved path and 7.5 rpm for the force-controlled path. The roller feed pitch was 1 mm / rev for the curved path and 0.5 mm / rev for the force-controlled path. The pushing force on the force-controlled path was 500 N. The forming took about 45 min under these conditions.

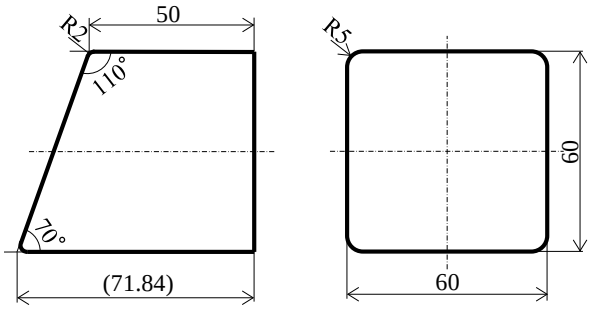

Figure 13 Mandrel for square cup with oblique bottom.

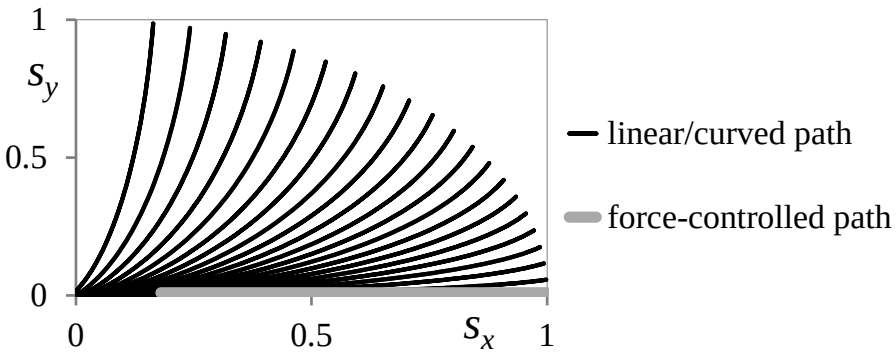

Figure 14　Normalized tool paths for square cup with oblique bottom.

Figure 15 shows a photograph of the formed product.　The edges of the side surface had bulges that were larger near the bottom.　In the neighborhood of the side edges, the flange due to the remainder of the material became large.　Because the roller moved in a different direction from the direction of rotation, the aluminum surface was peeled off in some places.

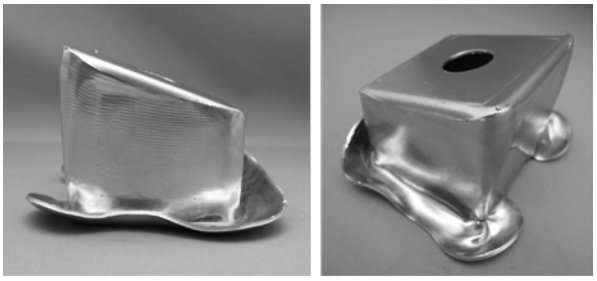

Figure 15　Photograph of formed product of square cup with oblique bottom.

Figure 16 shows the wall thickness distribution measured using a micrometer. Figure 17 shows the cross-section shape of the formed product. The cross section was measured at a product height of 20 mm from the center of the bottom. Figure 18 shows the axial profile of the product. The corner portion was measured for 40 mm in the axial direction. In Figure 16, 0°, 90°, and 180° correspond to the corners of the product, where the wall thickness was about 1.7 mm. Figure 17 also shows that the neighborhood of each corner was thicker than other parts. The material was concentrated at the corners while the planar blank was deformed along the square mandrel.

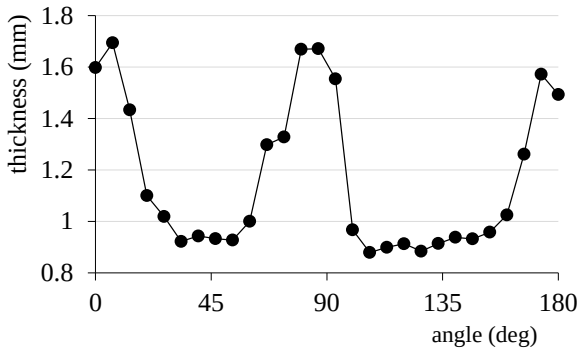

Figure 16 Wall thickness distribution of square cup with oblique bottom.

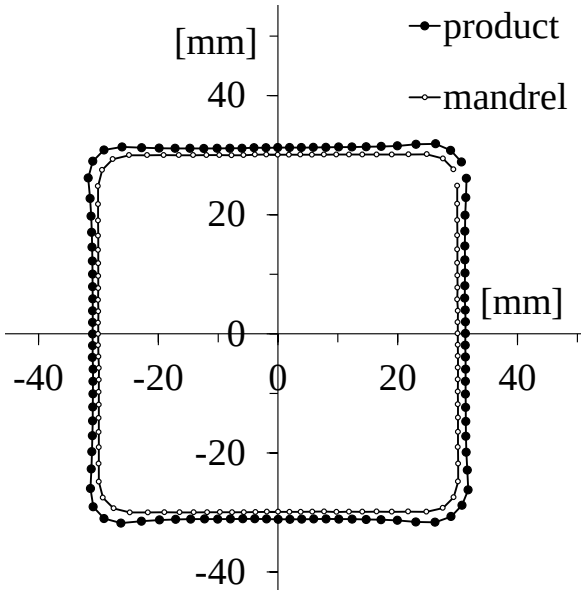

Figure 17　Cross-section profile of square cup with oblique bottom.

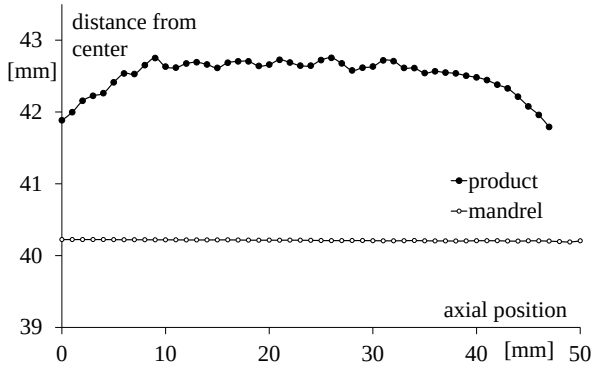

Figure 18　Axial profile of square cup with oblique bottom.

4. Calculation of tool trajectory using intermediate shape

In the forming experiment on a square cup with an oblique bottom in the previous section, the wall thickness was not uniform since the material was concentrated near the corners.　A similar phenomenon was observed in the forming of a square cup by synchronous multipass spinning by Sugita and

Arai (2014). To solve this problem, Arai (2015) proposed the use of an intermediate shape in the interpolation calculation of the tool trajectory.

A circular intermediate cross section $y = y_{mid}$ is defined at the outside of the cross section of the product. In the two-dimensional plane of the normalized tool path, $s_y = s_{mid}$ corresponds to the radial displacement y_{mid}. When s_y for the path is smaller than s_{mid}, the tool position is interpolated between the product shape and the intermediate shape. When s_y is larger than s_{mid}, the tool position is interpolated between the intermediate shape and the blank shape (Figure 19). As a result, the workpiece is formed as a cylindrical shape on the outside of the intermediate shape and then formed as a square shape on the inside of the intermediate shape. As the work is formed as a square shape via the cylindrical shape, the concentration of the material around the corners can be avoided.

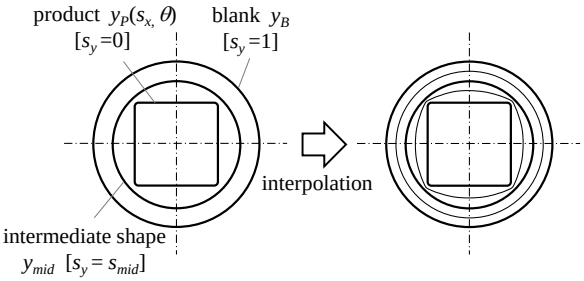

Figure 19 Interpolation of roller position in radial direction through intermediate circular cross section.

In this study, this method is expanded to adopt an inclined shape so as to solve the problem of material concentration near the corners. To use this method for an inclined shape, interpolation calculation using the intermediate shape is carried out in the axial direction as well as the radial direction as shown in Equations (8) and (9).

$$\begin{cases} x_t = \dfrac{s_y}{s_{mid}} x_{mid}(s_x,\theta) + \left(1 - \dfrac{s_y}{s_{mid}}\right) x_P(s_x,\theta) & (0 \le s_y < s_{mid}) \\ x_t = \left(1 - \dfrac{s_y - s_{mid}}{1 - s_{mid}}\right) x_{mid}(s_x,\theta) + \dfrac{s_y - s_{mid}}{1 - s_{mid}} x_b(s_x,\theta) & (s_{mid} \le s_y \le 1) \end{cases} \tag{8}$$

$$\begin{cases} y_t = \dfrac{s_y}{s_{mid}} y_{mid}(s_x,\theta) + \left(1 - \dfrac{s_y}{s_{mid}}\right) y_P(s_x,\theta) & (0 \le s_y < s_{mid}) \\ y_t = \left(1 - \dfrac{s_y - s_{mid}}{1 - s_{mid}}\right) y_{mid}(s_x,\theta) + \dfrac{s_y - s_{mid}}{1 - s_{mid}} y_b(s_x,\theta) & (s_{mid} \le s_y \le 1) \end{cases} \tag{9}$$

A square cup with an oblique bottom was spun by using an intermediate shape to find whether the concentration of the material near the corners can be moderated. Forming with and without the intermediate shape was conducted and the formed samples were compared.

The normalized forming path consisted of 20 roundtrip curved/linear paths and a force-controlled path (Figure 20), the feed pitch per rotation was 2 mm / rev, and the spindle rotation speed was 60 rpm. The interpolation coefficient s_{mid} was 0.2 in the intermediate circular cross section and y_{mid} was selected so that the diameter of the cross section was 102 mm. In

addition, the inclination of the cross section was gradually decreased to zero as the roller proceeds to the lower end of the mandrel.

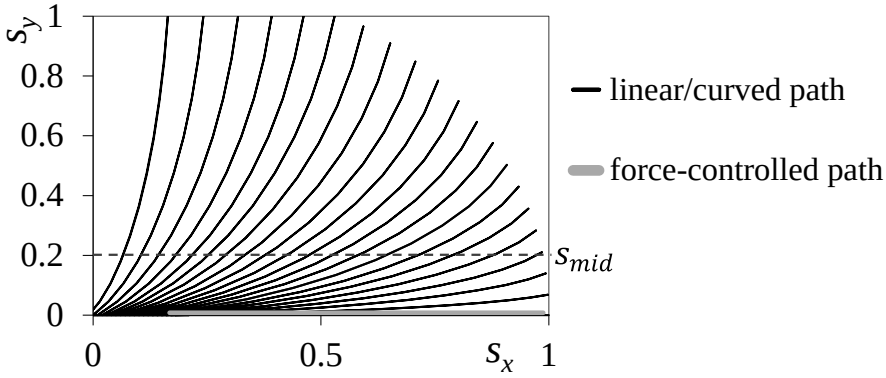

Figure 20 Normalized tool paths for spinning square cup with oblique bottom via intermediate shape.

Figure 21 shows photographs of the formed product using and without using the intermediate shape. When the intermediate shape was not used, the corners bulged and the flange only remains at the corners. This means that the material did not flow uniformly. In contrast, when the intermediate shape was used, the material flowed more uniformly and the bulge at the corners was decreased. Figure 22 shows the circumferential cross section of the product and Figure 23 shows the axial shape at a corner. The product formed without the intermediate shape had thin walls and thick corners. In contrast, Figure 22 indicates almost uniform thickness also near the corners. Also, the shape in the axial direction of Figure 23 had

nearly uniform thickness, while the shape without using the intermediate shape bulged considerably near the bottom and the lower end.

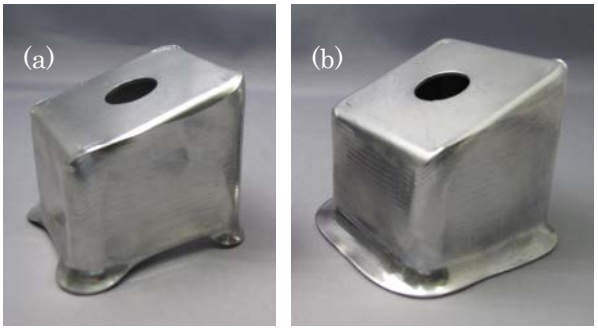

Figure 21　Photographs of square cups with oblique bottoms

(a) formed without using intermediate shape

(b) formed using intermediate shape.

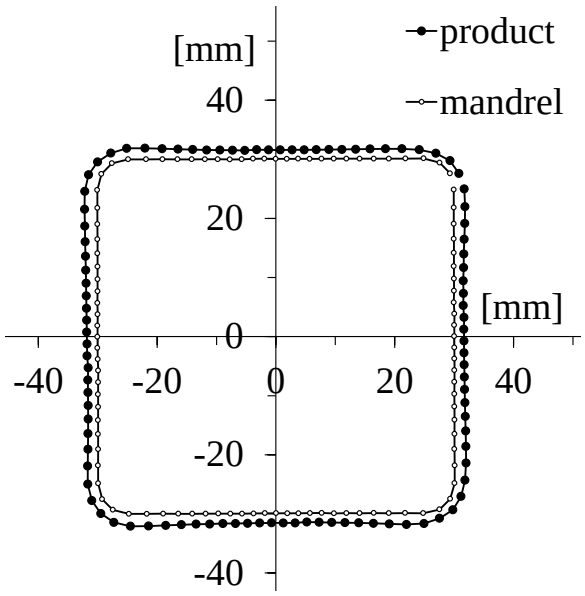

Figure 22　Cross-section profile of square cup with oblique bottom formed using intermediate shape.

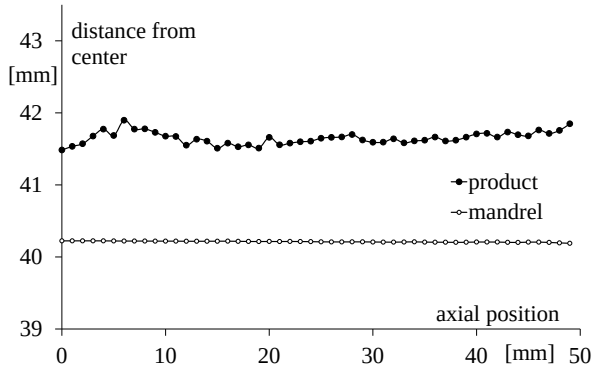

Figure 23　Axial profile of square cup with oblique bottom formed using intermediate shape.

The strain of the side surface of the product in the circumferential and axial direction was calculated by drawing markers along concentric circles on the back surface of the blank.　Figures 24 and 25 show the logarithmic strain at positions at a radius of 65 mm on the blank; 0° means the corner portion and 45° corresponds to the center of the side surface.　In the case of not using the intermediate shape (dotted line), the vicinity of the corner was greatly expanded in the axial direction and compressed in the circumferential direction.　On the other hand, it can be seen that the strains when using the intermediate shape were equalized in both the circumferential and radial directions.

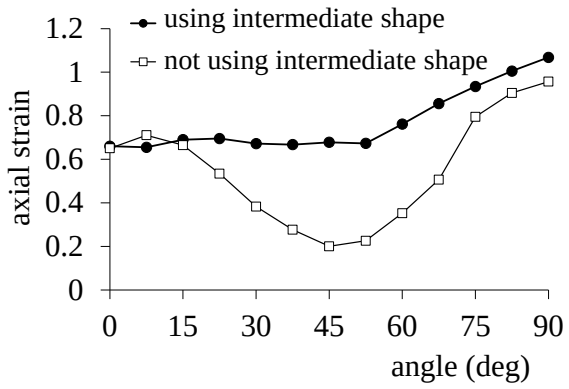

Figure 24　Axial strain of square cup with oblique bottom using and without using intermediate shape.

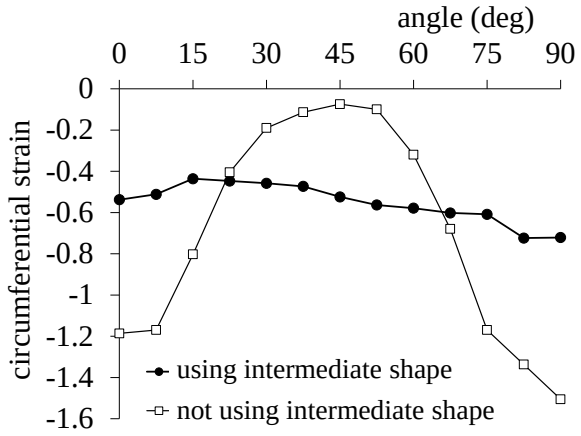

Figure 25　Circumferential strain of square cup with oblique bottom formed using and without using intermediate shape.

Owing to the inclination of the bottom surface, the axial strain also changes with the direction relative to the inclination.　90° corresponds to the acute angle side of the bottom surface, and the strain tended to increase

towards 90° in the cases both with and without the intermediate shape.

Figure 26 shows the thickness distribution at a distance of 20 mm from the bottom. 0° and 90° correspond to corners and 45° corresponds to the center of a side wall. In the case of not using the intermediate shape, the wall thickness near the corners was increased, while in the case of using the intermediate shape, the wall thickness at the corners was reduced and the wall thickness was equalized. It can be seen that the product formed using the intermediate shape tended to have rather small wall thicknesses as a whole.

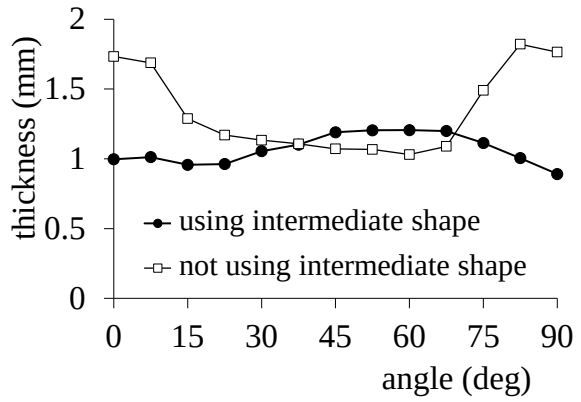

Figure 26 Thickness distribution of square cup with oblique bottom formed using and without using intermediate shape.

5. Effect of forming parameters

The effect of the process parameters, such as blank diameter, roller feed pitch, number of passes and pushing force, on the forming result was investigated, as reported in this section.

5.1 Blank diameter vs product height

In contrast to circular spinning, the products in this study have an uneven height at the lower end. It will be useful if an appropriate blank diameter can be chosen to form the target shape. A forming experiment was conducted to investigate the relationship between the blank diameter and the height of the product.

Cylindrical cups and oblique square cups with an oblique bottom were spun from blanks of different diameters. Square cups with a non-oblique bottom were also spun for comparison. The square cups were spun without using the intermediate shape in Section 4. Table 1 shows the blank diameters for each shape. Figures 27 – 29 show photographs of the products spun from the blanks of different diameters.

Table 1　Blank diameters of formed shapes

Product shape	Blank diameter
Cylindrical cup with oblique bottom	120, 130, 140, 150 (mm)
Square cup with oblique bottom	110, 120, 130, 140 (mm)
Square cup with non-oblique bottom	110, 120, 130, 140 (mm)

Figure 27　Cylindrical cups with oblique bottom spun from blanks of different diameters.

Figure 28　Square cups with oblique bottom spun from blanks of different diameters.

Figure 29　Square cups with non-oblique bottom spun from blanks of different diameters.

For the cups with an oblique bottom, the minimum heights of the side walls on the acute-angle side (70°) and obtuse-angle side (110°) were measured (Figure 30). For the square cups with a non-oblique bottom, the minimum heights of the side walls were averaged. Figures 31 – 33 show plots of the side wall height for each blank diameter.

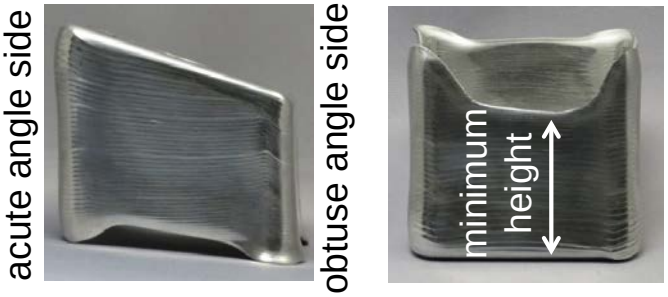

Figure 30　Measurement of side wall height of square cup.

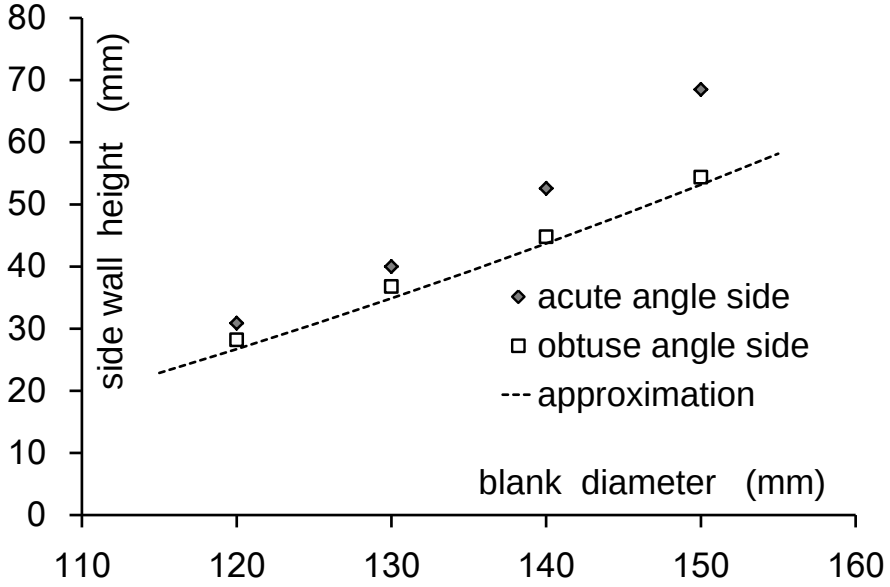

Figure 31 Side wall height of cylindrical cups with oblique bottom spun from blanks of different diameters.

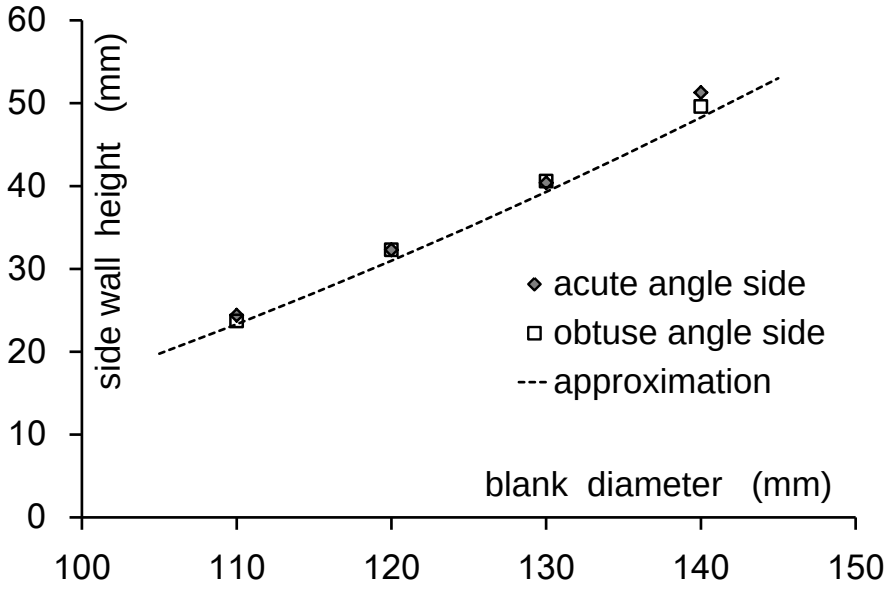

Figure 32 Side wall height of square cups with oblique bottom spun from blanks of different diameters.

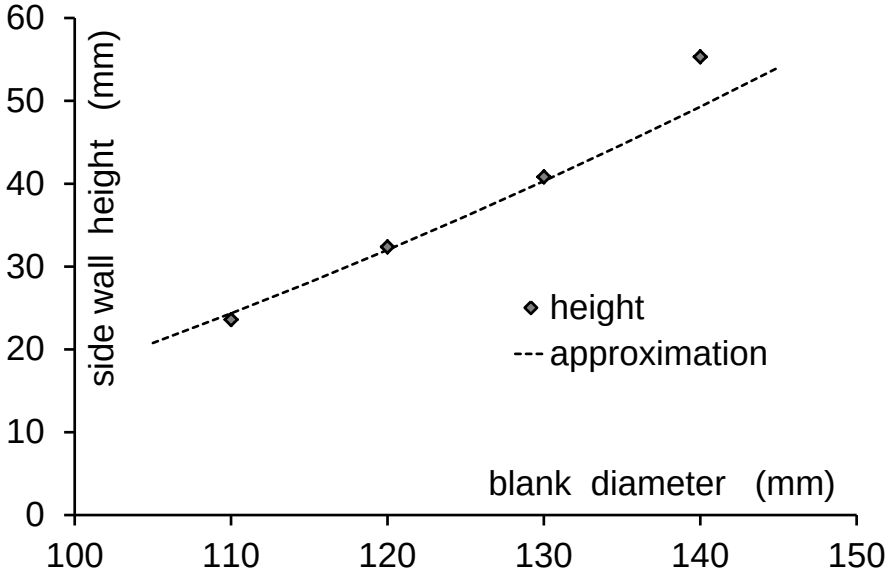

Figure 33 Side wall height of square cups with non-oblique bottom spun from blanks of different diameters.

The side wall height was roughly estimated using the following simple assumptions: i) the surface area of the product is equal to the area of the blank, ii) the side wall has a uniform height from the upper end to the lower end. The area of the blank S_0 is $S_0 = \frac{\pi D^2}{4}$, where D is the diameter of the blank. The area of the bottom of the oblique cylindrical cup is $S_1 = \frac{\pi(d+t)^2}{4\cos\theta}$, where d is the diameter of the mandrel, t is the blank thickness and θ is the inclination angle. The area of the bottom of the oblique square cup is $S_1 = \frac{(d+t)^2 - \left(1-\frac{\pi}{4}\right)(2r+t)^2}{\cos\theta}$, where d is the width of the mandrel and r is the radius of roundness at the mandrel edge. The circumferential length of the cylindrical cup is $L = \pi(d+t)$. The circumferential length of the square

cup is $L = 4(d + t) - (4 - \pi)(2r - t)$. The height of the side wall is calculated as $h = \frac{S_0 - S_1}{L}$.

The broken lines in Figures 31 – 33 show the estimated height. It is observed that this simple estimation gives a good approximation of the side wall height of the oblique and non-oblique square cups, although the acute-angle side wall of the oblique circular cups are somewhat higher than the estimated values.

5.2 Roller feed pitch and number of passes vs forming limit

Next, the forming limit was investigated in terms of the number of passes and the roller feed pitch of the curved/linear path. The number of passes was 10, 15, 20 or 25. The roller feed pitch was 1mm, 2mm, 3mm or 4mm. Square cups with oblique and non-oblique bottoms were spun using various combinations of these two parameters. The oblique square cups were formed with and without using the intermediate shape. The success and failure of the forming results are illustrated in Figures 34 – 36. All of the failure cases for these parameters were due to wrinkles and no fracture was observed. Figure 37 shows examples of failed workpieces for the square cup with an oblique bottom.

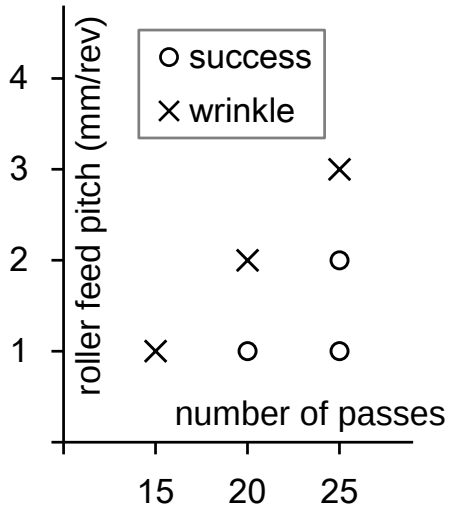

Figure 34　Forming limit of square cup with oblique bottom without using intermediate shape.

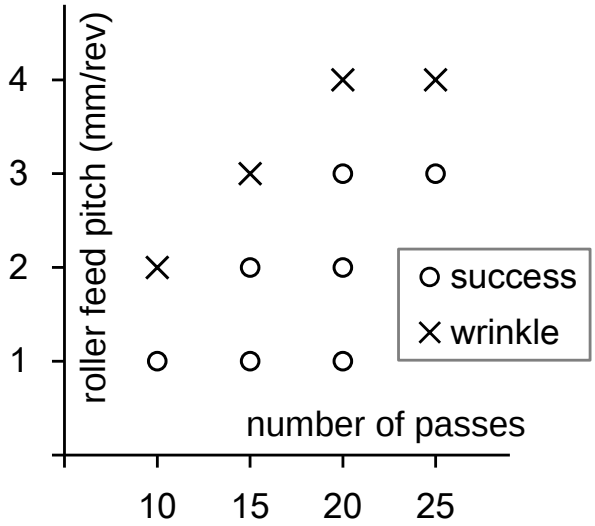

Figure 35　Forming limit of square cup with oblique bottom using intermediate shape.

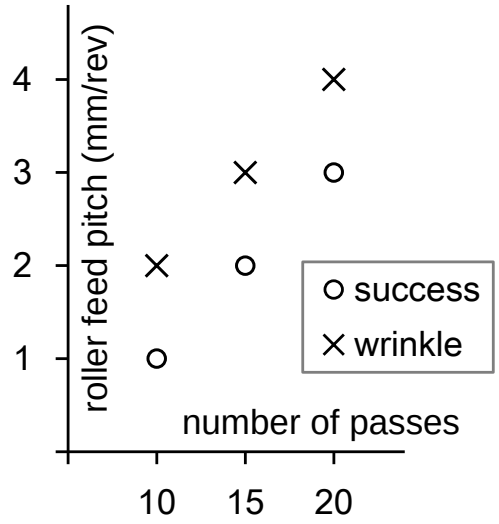

Figure 36　Forming limit of square cup with non-oblique bottom.

20 passes, 2mm/rev
without intermediate shape

10 passes, 2mm/rev
with intermediate shape

Figure 37　Failed workpieces of square cup with oblique bottom.

Wrinkles were more likely to occur as the number of passes decreased and the roller feed pitch increased.　In the case of the oblique square cups, most wrinkles originated from buckling at the flange on the acute-angle side. The oblique square cups much more easily failed than the non-oblique

square cups. However, when the intermediate shape was applied for the oblique square cups, the occurrence of wrinkles was prevented and the process window became much wider. The intermediate shape resulted in a uniform circular flange in the early stage of the process, and the buckling at the edge of the workpiece was suppressed.

5.3 Pushing force and roller feed pitch vs forming accuracy

Finally, the effect of the pushing force and the roller feed pitch of the force-controlled path on the forming accuracy of the product shape was investigated. A square cup with an oblique bottom was spun using the intermediate shape. The pushing force of the final pass was 250N, 375N, 500N, 625N or 750N while the roller feed pitch of the path was 1mm/rev. The cross section of the product was measured at a height of 30 mm from the center of its bottom using a laser distance sensor. Figure 38 shows the circumferential profile of the acute-angle side for the pushing forces of 250N and 750N. The pushing force of 250N was insufficient and there was a gap between the product and the mandrel around the corner edge. When the pushing force was 750N, the product tightly fitted the mandrel. Figure 39 plots the averaged distance of the product surface from the mandrel surface at a flat section of the acute-angle side. As the pushing force increased, the distance decreased to nearly the wall thickness.

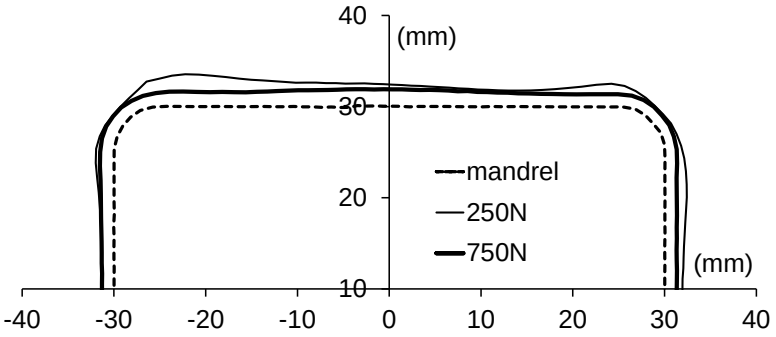

Figure 38　Change in product profile with pushing force.

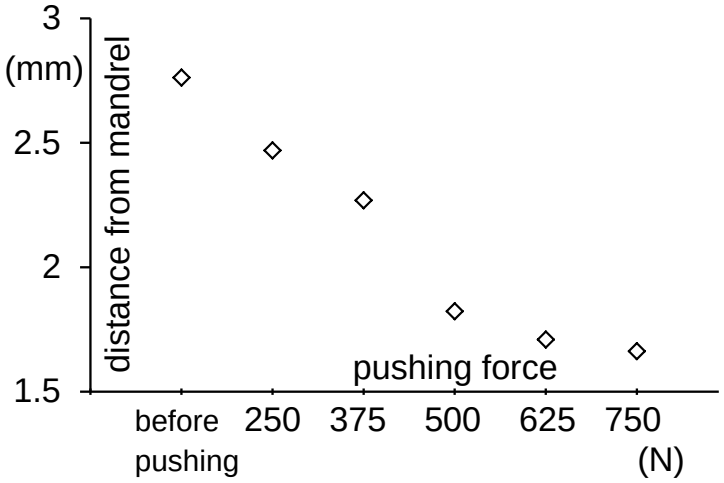

Figure 39　Change in distance between product surface and mandrel surface with pushing force.

Then, the roller feed pitch was set to 0.5mm/rev, 1mm/rev, 1.5mm/rev or 2mm/rev while the pushing force was fixed to 500N.　Figure 40 shows the distance between the product and the mandrel.　The distance increased as the roller feed pitch increased, but its effect on the distance was weaker than that of the pushing force.　In addition to spoiling the forming accuracy, a

large roller feed pitch deteriorated the flatness of the product surface because of the feed mark of the roller.

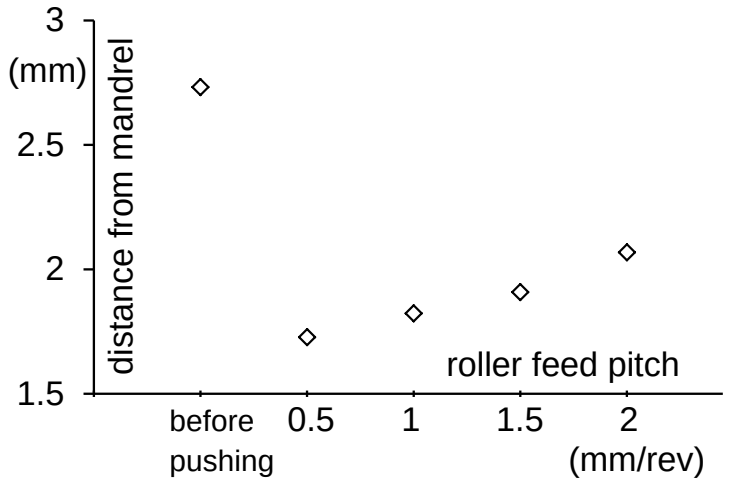

Figure 40　Change in distance between product surface and mandrel surface with roller feed pitch.

6. Conclusions

Noncircular shapes with oblique bottoms and vertical walls are formed by synchronous multipass spinning.　The conclusions of this paper are as follows:

(1) The tool trajectory can be obtained by interpolation of the inclined product shape and the blank shape, using the normalized tool path as the interpolation coefficient.　The roller is synchronized with the spindle rotation in both the axial and radial directions to track the inclined

forming plane.

(2) A cylindrical cup and square cup with an oblique bottom and vertical side walls are successfully spun from pure aluminum sheets using the proposed method. The workpiece fits each mandrel and the target shape is obtained without wrinkles or fractures.

(3) The material is concentrated near the side edges of the square cup, where the thickness is increased more than in other areas. The neighborhood of each corner is greatly expanded in the axial direction and compressed in the circumferential direction.

(4) The intermediate circular shape used in the interpolation of the tool trajectory can moderate the local concentration of the material at the side edges of the square cup. The square cup is formed via the intermediate circular cross section and the difference in the wall thickness is decreased.

(5) The height of the side wall of the product can be roughly estimated by assuming that the surface area of the product equals that of the blank and that the height is uniform.

(6) The number of passes and the roller feed pitch of the curved paths determine the forming limit due to wrinkles. Wrinkles occur when the number of passes is too small and the roller feed pitch is too large. The

forming limit of an oblique square cup is lower than that of a non-oblique square cup. When the intermediate shape is used for an oblique square cup, the forming limit increases.

(7) When the pushing force of the force-controlled path is increased, the product tightly fits the mandrel and the forming accuracy is improved.

This research did not receive any specific grant from funding agencies in the public, commercial, or not-for-profit sectors.

References

Amano, T., Tamura, K., 1984. The study of an elliptical cone spinning by the trial equipment. In: Proceedings of the Third International Conference on Rotary Metalworking Processes, Kyoto, Japan, pp. 213–224.

Xia, Q., Lai, Z., Zhan, X., Cheng, X., 2010. Research on Spinning Method of Hollow Part with Triangle Arc-Type Cross Section Based on Profiling Driving, Steel Research International 81 (9), pp. 994–998.

Shimizu, I., 2010. Asymmetric forming of aluminum sheets by synchronous spinning. J. Mater. Process. Technol. 210, pp. 585–592.

Arai, H., Okazaki, I., Fujimura, S., 2005. Synchronized metal spinning of non-axisymmetric tubes. In: Proceedings of 56th Japanese Joint Conference for the Technology of Plasticity, Naha, Japan, pp. 687–688. (in Japanese)

Awiszus, B., Meyer, F., 2005. Metal spinning of non-circular hollow parts. In:Proceedings of 8th ICTP, Verona, Italy, pp. 353–355.

Arai, H., 2005. Robotic metal spinning – Forming asymmetric products using force control. In: Proceedings of 2005 IEEE International Conference on Robotics and Automation, Barcelona, Spain, pp. 2702–2707.

Arai, H., 2006. Force-controlled metal spinning machine using linear motors. In: Proceedings of the 2006 IEEE International Conference on Robotics

and Automation, Orlando, Florida, pp. 4031–4036.

Härtel, S., Laue, R., 2016. An optimization approach in non-circular spinning, J. Mater. Process. Technol. 229, pp. 417–430.

Sugita, Y., Arai, H., 2015. Formability in synchronous multipass spinning using simple pass set, J. Mater. Process. Technol. 217, pp. 336–344.

Arai, H., 2013. Metal spinning technology to form noncircular shapes, Press Working 51(11), pp. 92–95. (in Japanese)

Sugita, Y., Arai, H., 2011. Forming a cup with re-entrant contour by synchronous multi-pass metal spinning, In: Proceedings of 62th Japanese Joint Conference for the Technology of Plasticity, Toyohashi, Japan, pp. 415–416. (in Japanese)

Music, O., Allwood, J., 2011. Flexible asymmetric spinning, CIRP Annals - Manufacturing Technology, 60(1), pp. 319–322.

Irie,T., 2001. Method and apparatus for forming a processed portion of a workpiece. United States Patent, US6223993B1, May 22, 2001.

Xia, Q., Cheng, X., Long, H., Ruan, F., 2012. Finite element analysis and experimental investigation on deformation mechanism of non-axisymmetric tube spinning, Int. J. Adv. Manuf. Technol., 59 (1–4), pp. 263–272.

Sekiguchi, A., Arai, H., 2010. Synchronous die-less spinning of curved

products. Steel Research International, 81 (9), pp. 1010–1013.

Arai, H., 2015. Equalization of Material Flow in Multipass Synchronous Spinning of Square Cup, J. Japan Society for Technology of Plasticity, 56 (656), pp. 787–792. (in Japanese)